

Advection of nematic liquid crystals by chaotic flow

Lennon Ó Náraigh

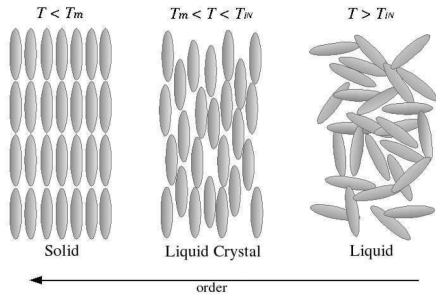
School of Mathematics and Statistics and the Institute for Discovery,
University College Dublin, Ireland

Tuesday 7th February 2017

Context of work

Liquid crystals are rodlike molecules that possess an intermediate phase between solid and liquid, hence two melting points:

- A 'lower' melting point T_m : the substance is solid for $T < T_m$;
- An 'upper' melting point T_{IN} : the substance behaves like an isotropic liquid for $T > T_{IN}$

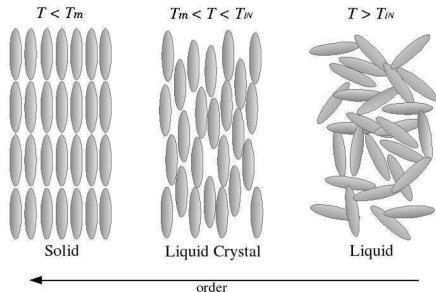


Context of work

Liquid crystals are rodlike molecules that possess an intermediate phase between solid and liquid, hence two melting points:

- A 'lower' melting point T_m : the substance is solid for $T < T_m$;
- An 'upper' melting point T_{IN} : the substance behaves like an isotropic liquid for $T > T_{IN}$

Between these values, the substance has orientational order and behaves like a fluid with a highly complicated rheology – **liquid crystal**.



Context of work

Liquid crystals aligned in a single direction have the same optical properties as uniaxial crystals, yet their properties are easily modified by outside influences (e.g. electrical fields, strain fields, etc.), hence their ubiquity in LCDs.



Another way to modify liquid crystal properties – **hydrodynamics** – the main focus of this talk.

Modelling Approach

The **director** $\hat{\mathbf{n}}(\mathbf{x}, t)$ gives the mesoscopically-averaged direction of molecular orientation at a point \mathbf{x} . Necessary to formulate evolution equations for $\hat{\mathbf{n}}(\mathbf{x}, t)$.

Modelling Approach

The **director** $\hat{\mathbf{n}}(\mathbf{x}, t)$ gives the mesoscopically-averaged direction of molecular orientation at a point \mathbf{x} . Necessary to formulate evolution equations for $\hat{\mathbf{n}}(\mathbf{x}, t)$.

Molecules have head-tail symmetry, so it's better to formulate the equations in terms of a symmetric, traceless **Q-tensor**, where

$$Q_{ij} = (2\lambda_1 + \lambda_2) \left(n_i^{(1)} n_j^{(1)} - \frac{1}{3} \delta_{ij} \right) + (2\lambda_2 + \lambda_1) \left(n_i^{(2)} n_j^{(2)} - \frac{1}{3} \delta_{ij} \right).$$

Modelling Approach

The **director** $\hat{\mathbf{n}}(\mathbf{x}, t)$ gives the mesoscopically-averaged direction of molecular orientation at a point \mathbf{x} . Necessary to formulate evolution equations for $\hat{\mathbf{n}}(\mathbf{x}, t)$.

Molecules have head-tail symmetry, so it's better to formulate the equations in terms of a symmetric, traceless **Q-tensor**, where

$$Q_{ij} = (2\lambda_1 + \lambda_2) \left(n_i^{(1)} n_j^{(1)} - \frac{1}{3} \delta_{ij} \right) + (2\lambda_2 + \lambda_1) \left(n_i^{(2)} n_j^{(2)} - \frac{1}{3} \delta_{ij} \right).$$

If $2\lambda_2 + \lambda_1 = 0$ then the Q-tensor has a 'familiar' form,

$$Q_{ij} = \frac{1}{2} S \left(n_i^{(1)} n_j^{(1)} - \frac{1}{3} \delta_{ij} \right), \quad S = \sqrt{6 \text{tr}(\mathbf{Q}^2)} = 3\lambda_1 \quad (\text{scalar } \mathbf{order \ parameter})$$

and the eigenvector can be unambiguously identified with the direction of the (ahem) director – rodlike molecule – **uniaxial case**.

Modelling Approach

The **director** $\hat{\mathbf{n}}(\mathbf{x}, t)$ gives the mesoscopically-averaged direction of molecular orientation at a point \mathbf{x} . Necessary to formulate evolution equations for $\hat{\mathbf{n}}(\mathbf{x}, t)$.

Molecules have head-tail symmetry, so it's better to formulate the equations in terms of a symmetric, traceless **Q-tensor**, where

$$Q_{ij} = (2\lambda_1 + \lambda_2) \left(n_i^{(1)} n_j^{(1)} - \frac{1}{3} \delta_{ij} \right) + (2\lambda_2 + \lambda_1) \left(n_i^{(2)} n_j^{(2)} - \frac{1}{3} \delta_{ij} \right).$$

If $2\lambda_2 + \lambda_1 = 0$ then the Q-tensor has a 'familiar' form,

$$Q_{ij} = \frac{1}{2} S \left(n_i^{(1)} n_j^{(1)} - \frac{1}{3} \delta_{ij} \right), \quad S = \sqrt{6 \text{tr}(\mathbf{Q}^2)} = 3\lambda_1 \quad (\text{scalar } \mathbf{order \ parameter})$$

and the eigenvector can be unambiguously identified with the direction of the (ahem) director – rodlike molecule – **uniaxial case**.

For the general case, there are three directions associated with the Q-tensor – ellipsoidal molecule (**biaxial** liquid crystal).

Landau theory

Landau theory is applied to the system near the liquid/liquid-crystal transition temperature, writing the free energy of the system as

$$F = F_0 + F_K,$$

where F_0 is the double-well part associated with the phase change:

$$F_0 = \int d^3x \chi(\mathbf{Q}), \quad \chi(\mathbf{Q}) = \frac{1}{2} \alpha_F \text{tr}(\mathbf{Q}^2) - \beta_F \text{tr}(\mathbf{Q}^3) + \gamma_F [\text{tr}(\mathbf{Q}^2)]^2,$$
$$\alpha_F = 12a(T - T_*).$$

The term F_K is the energy penalty for distortions,

$$F_K = \int d^3x W(\nabla \mathbf{Q}), \quad W(\nabla \mathbf{Q}) = \frac{1}{2} k \|\nabla \mathbf{Q}\|_2^2$$

under the one-elastic-constant assumption (bend, splay, and twist all energetically equally unfavourable).

Structure of quartic potential, uni-axial case

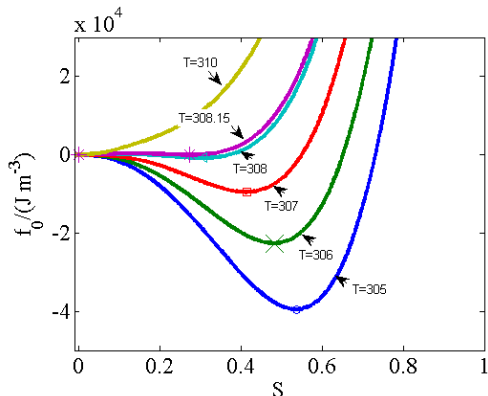
In the absence of inhomogeneities, the structure of the quartic potential $\chi(\mathbf{Q})$ can be understood using

$$\chi(S) = \frac{1}{12}\alpha_F S^2 - \underbrace{\frac{1}{36}\beta_F}_{=B} S^3 + \underbrace{\frac{1}{36}\gamma_F}_{=C} S^3, \quad S = \sqrt{6 \operatorname{tr}(\mathbf{Q}^2)}, \quad Q_{ij} \text{ uniaxial}$$

- Free-energy minima
 $(\partial\chi/\partial S)_{S_*} = 0$
- Nematic state favourable compared to isotropic one:
 $\chi(S_*, T) < \chi(0, T)$
- Gives critical temperature

$$T_{IN} = T_* + \frac{B^2}{4ac},$$

where $\alpha_F = 12a(T - T_*)$.



Gradient dynamics

With inhomogeneities present, but without flow, system evolves so as to minimize its free energy – subject to the constraint (Lagrange multiplier) that the Q -tensor remains traceless. Result –

$$\zeta_1 \frac{\partial Q_{ij}}{\partial t} = - \left[\frac{\delta F}{\delta Q_{ij}} - \frac{1}{3} \text{tr} \left(\frac{\delta F}{\delta Q_{ij}} \right) \delta_{ij} \right].$$

Coupling to incompressible flow – continuum mechanics I

- Write down Lagrangian for incompressible flow, constant density ρ_0 :

$$L = \int_{\Omega} d^3a \left\{ \frac{1}{2} \left(\frac{\partial \mathbf{x}}{\partial t} \right)^2 + \left(1 - \frac{\rho}{\rho_0} \right) \frac{p}{\rho_0} \right\} - \int_{\Omega} \frac{d^3a}{\rho_0} [\chi(\mathbf{Q}) + W(\mathbf{Q}) - \lambda \mathbf{Q} \cdot \mathbb{I}]$$

where \mathbf{a} is a particle label and $\rho_0 d^3x = d^3a$.

Coupling to incompressible flow – continuum mechanics I

- Write down Lagrangian for incompressible flow, constant density ρ_0 :

$$L = \int_{\Omega} d^3a \left\{ \frac{1}{2} \left(\frac{\partial \mathbf{x}}{\partial t} \right)^2 + \left(1 - \frac{\rho}{\rho_0} \right) \frac{p}{\rho_0} \right\} - \int_{\Omega} \frac{d^3a}{\rho_0} [\chi(\mathbf{Q}) + W(\mathbf{Q}) - \lambda \mathbf{Q} \cdot \mathbb{I}]$$

where \mathbf{a} is a particle label and $\rho_0 d^3x = d^3a$.

- The generalized forces are

$$\mathbf{F}_{\mathbf{v}} = \frac{\partial}{\partial \tau} \frac{\delta L}{\delta(\partial \mathbf{x} / \partial \tau)} - \frac{\delta L}{\delta \mathbf{x}}, \quad \mathbf{F}_{\mathbf{Q}} = \frac{\partial}{\partial \tau} \frac{\delta L}{\delta(\partial \mathbf{Q} / \partial \tau)} - \frac{\delta L}{\delta \mathbf{Q}},$$

where $\mathbf{v} = \partial \mathbf{x} / \partial \tau$ is the velocity of a Lagrangian particle.

Coupling to incompressible flow – continuum mechanics I

- Write down Lagrangian for incompressible flow, constant density ρ_0 :

$$L = \int_{\Omega} d^3a \left\{ \frac{1}{2} \left(\frac{\partial \mathbf{x}}{\partial t} \right)^2 + \left(1 - \frac{\rho}{\rho_0} \right) \frac{p}{\rho_0} \right\} - \int_{\Omega} \frac{d^3a}{\rho_0} [\chi(\mathbf{Q}) + W(\mathbf{Q}) - \lambda \mathbf{Q} \cdot \mathbb{I}]$$

where \mathbf{a} is a particle label and $\rho_0 d^3x = d^3a$.

- The generalized forces are

$$\mathbf{F}_{\mathbf{v}} = \frac{\partial}{\partial \tau} \frac{\delta L}{\delta(\partial \mathbf{x} / \partial \tau)} - \frac{\delta L}{\delta \mathbf{x}}, \quad \mathbf{F}_{\mathbf{Q}} = \frac{\partial}{\partial \tau} \frac{\delta L}{\delta(\partial \mathbf{Q} / \partial \tau)} - \frac{\delta L}{\delta \mathbf{Q}},$$

where $\mathbf{v} = \partial \mathbf{x} / \partial \tau$ is the velocity of a Lagrangian particle.

- Dissipation is accounted for by dissipative forces; these are $-\delta \mathcal{R} / \delta \mathbf{v}$ and $-\delta \mathcal{R} / \delta \mathbf{Q}$, where \mathcal{R} is a dissipative function, to be modelled.

Coupling to incompressible flow – continuum mechanics I

- Write down Lagrangian for incompressible flow, constant density ρ_0 :

$$L = \int_{\Omega} d^3a \left\{ \frac{1}{2} \left(\frac{\partial \mathbf{x}}{\partial t} \right)^2 + \left(1 - \frac{\rho}{\rho_0} \right) \frac{p}{\rho_0} \right\} - \int_{\Omega} \frac{d^3a}{\rho_0} [\chi(\mathbf{Q}) + W(\mathbf{Q}) - \lambda \mathbf{Q} \cdot \mathbb{I}]$$

where \mathbf{a} is a particle label and $\rho_0 d^3x = d^3a$.

- The generalized forces are

$$\mathbf{F}_{\mathbf{v}} = \frac{\partial}{\partial \tau} \frac{\delta L}{\delta(\partial \mathbf{x} / \partial \tau)} - \frac{\delta L}{\delta \mathbf{x}}, \quad \mathbf{F}_{\mathbf{Q}} = \frac{\partial}{\partial \tau} \frac{\delta L}{\delta(\partial \mathbf{Q} / \partial \tau)} - \frac{\delta L}{\delta \mathbf{Q}},$$

where $\mathbf{v} = \partial \mathbf{x} / \partial \tau$ is the velocity of a Lagrangian particle.

- Dissipation is accounted for by dissipative forces; these are $-\delta \mathcal{R} / \delta \mathbf{v}$ and $-\delta \mathcal{R} / \delta \mathbf{Q}$, where \mathcal{R} is a dissipative function, to be modelled.
- Theory is closed by equating dissipative forces with generalized forces:

$$\frac{\partial}{\partial \tau} \frac{\delta L}{\delta(\partial \mathbf{x} / \partial \tau)} - \frac{\delta L}{\delta \mathbf{x}} = -\frac{\delta \mathcal{R}}{\delta \mathbf{v}} \text{ etc.}$$

Coupling to incompressible flow – continuum mechanics II

Dissipation is modelled so as to be a positive-definite materially frame-indifferent quantity. Also, should reduce to Navier–Stokes when $\mathbf{Q} \rightarrow 0$. Hence,

$$\mathcal{R} = \frac{1}{\rho_0} \int_{\Omega} d^3a R,$$

where R is a quadratic function of \mathbf{D} (strain rate) and the **co-rotational derivative**

$$\overset{\circ}{\mathbf{Q}} = \frac{\partial \mathbf{Q}}{\partial t} + \mathbf{v} \cdot \nabla \mathbf{Q} - \boldsymbol{\Omega} \mathbf{Q} + \mathbf{Q} \boldsymbol{\Omega}, \quad \Omega_{ij} = \frac{1}{2} (\partial_i u_j - \partial_j u_i),$$

hence

$$R = R(\mathbf{D}, \mathbf{Q}, \overset{\circ}{\mathbf{Q}}).$$

Final version of equations

Putting this all together, with

$$R = \frac{1}{2}\zeta_1 = \dot{\mathbf{Q}} \cdot \dot{\mathbf{Q}} + \zeta_2 \mathbf{D} \cdot \dot{\mathbf{Q}} + \frac{1}{2}\zeta_3 \mathbf{D} \cdot \mathbf{D} + \frac{1}{2}\zeta_{31} \mathbf{D} \cdot (\mathbf{D}\mathbf{Q}) + \frac{1}{2}\zeta_{32} (\mathbf{D} \cdot \mathbf{Q})^2,$$
$$\mathbf{D} \cdot \mathbf{Q} = D_{ij}Q_{ij} \text{ etc.}$$

gives a final set of equations:

Final version of equations

Putting this all together, with

$$R = \frac{1}{2}\zeta_1 = \dot{\mathbf{Q}} \cdot \dot{\mathbf{Q}} + \zeta_2 \mathbf{D} \cdot \dot{\mathbf{Q}} + \frac{1}{2}\zeta_3 \mathbf{D} \cdot \mathbf{D} + \frac{1}{2}\zeta_{31} \mathbf{D} \cdot (\mathbf{D}\mathbf{Q}) + \frac{1}{2}\zeta_{32} (\mathbf{D} \cdot \mathbf{Q})^2,$$

$$\mathbf{D} \cdot \mathbf{Q} = D_{ij} Q_{ij} \text{ etc.}$$

gives a final set of equations:

Q-tensor: $\zeta_1 \left(\frac{\partial \mathbf{Q}}{\partial t} + \mathbf{v} \cdot \nabla \mathbf{Q} - \boldsymbol{\Omega} \mathbf{Q} - \mathbf{Q} \boldsymbol{\Omega} \right) + \underbrace{\zeta_2 \mathbf{D}}_{\text{Note inhomogeneity!}} =$

$$k \nabla^2 \mathbf{Q} - (\alpha_F \mathbf{Q} - 3\beta_F \mathbf{Q}^2 + 4\gamma_F \text{tr}(\mathbf{Q}^2) \mathbf{Q}) + \frac{1}{3} \mathbb{I} [\zeta_2 \text{tr}(\mathbf{D}) - 3\beta_F \text{tr}(\mathbf{Q}^2)],$$

Hydrodynamics: $\rho_0 \left(\frac{\partial \mathbf{v}}{\partial t} + \mathbf{v} \cdot \nabla \mathbf{v} \right) = \nabla \cdot \mathbf{T},$

$$\mathbf{T} = -p \mathbb{I} - k \nabla \mathbf{Q} \odot \nabla \mathbf{Q} + \zeta_2 \dot{\mathbf{Q}} + \zeta_3 \mathbf{D} + \zeta_{31} (\mathbf{D}\mathbf{Q} + \mathbf{Q}\mathbf{D}) + \zeta_{32} (\mathbf{D} \cdot \mathbf{Q}) \mathbf{Q},$$

Incompressibility: $\nabla \cdot \mathbf{v} = 0.$

Non-dimensional equations – dimensionless groups

Length scale L and timescale $t_0 = \zeta_1 / (8\gamma_F)$ – hence dimensionless Q-tensor equation

$$\begin{aligned} \frac{\partial \mathbf{Q}}{\partial \tilde{t}} + \tilde{\mathbf{v}} \cdot \tilde{\nabla} \mathbf{Q} - \tilde{\boldsymbol{\Omega}} \mathbf{Q} - \mathbf{Q} \tilde{\boldsymbol{\Omega}} + \underbrace{\text{Tu}}_{=(\zeta_2/\zeta_1)} \tilde{\mathbf{D}} \\ = \epsilon^2 \tilde{\nabla}^2 \mathbf{Q} + g_1(1-\theta) \mathbf{Q} + 3g_2 \mathbf{Q}^2 - \frac{1}{2} \text{tr}(\mathbf{Q}^2) \mathbf{Q} + \frac{1}{3} \mathbb{I} \left[\text{Tu tr}(\tilde{\mathbf{D}}) - 3g_2 \text{tr}(\mathbf{Q}^2) \right], \end{aligned}$$

where

Non-dimensional equations – dimensionless groups

Length scale L and timescale $t_0 = \zeta_1 / (8\gamma_F)$ – hence dimensionless Q-tensor equation

$$\begin{aligned} \frac{\partial \mathbf{Q}}{\partial \tilde{t}} + \tilde{\mathbf{v}} \cdot \tilde{\nabla} \mathbf{Q} - \tilde{\boldsymbol{\Omega}} \mathbf{Q} - \mathbf{Q} \tilde{\boldsymbol{\Omega}} + \underbrace{\mathbf{Tu}}_{=(\zeta_2/\zeta_1)} \tilde{\mathbf{D}} \\ = \epsilon^2 \tilde{\nabla}^2 \mathbf{Q} + g_1(1-\theta) \mathbf{Q} + 3g_2 \mathbf{Q}^2 - \frac{1}{2} \text{tr}(\mathbf{Q}^2) \mathbf{Q} + \frac{1}{3} \mathbb{I} \left[\mathbf{Tu} \text{tr}(\tilde{\mathbf{D}}) - 3g_2 \text{tr}(\mathbf{Q}^2) \right], \end{aligned}$$

where

$$\alpha_F / (8\gamma_F) = -g_1 [1 - (T/T_*)] \equiv -g_1(1-\theta), \quad \beta_F / (8\gamma_F) = g_2, \quad \epsilon = k / (L^2 \gamma_F).$$

Non-dimensional equations – dimensionless groups

Length scale L and timescale $t_0 = \zeta_1 / (8\gamma_F)$ – hence dimensionless Q-tensor equation

$$\begin{aligned} \frac{\partial \mathbf{Q}}{\partial \tilde{t}} + \tilde{\mathbf{v}} \cdot \tilde{\nabla} \mathbf{Q} - \tilde{\Omega} \mathbf{Q} - \mathbf{Q} \tilde{\Omega} + \underbrace{\mathbf{Tu}}_{=(\zeta_2/\zeta_1)} \tilde{\mathbf{D}} \\ = \epsilon^2 \tilde{\nabla}^2 \mathbf{Q} + g_1(1-\theta) \mathbf{Q} + 3g_2 \mathbf{Q}^2 - \frac{1}{2} \text{tr}(\mathbf{Q}^2) \mathbf{Q} + \frac{1}{3} \mathbb{I} \left[\mathbf{Tu} \text{tr}(\tilde{\mathbf{D}}) - 3g_2 \text{tr}(\mathbf{Q}^2) \right], \end{aligned}$$

where

$$\alpha_F / (8\gamma_F) = -g_1 [1 - (T/T_*)] \equiv -g_1(1-\theta), \quad \beta_F / (8\gamma_F) = g_2, \quad \epsilon = k / (L^2 \gamma_F).$$

Hence also, a dimensionless momentum equation:

$$\frac{\partial \tilde{\mathbf{v}}}{\partial \tilde{t}} + \tilde{\mathbf{v}} \cdot \tilde{\nabla} \tilde{\mathbf{v}} = -\tilde{\nabla} \tilde{p} + \frac{1}{\text{Re}} \nabla \cdot \tilde{\mathbf{D}} + \text{Br} \nabla \cdot \left[-\epsilon^2 \tilde{\nabla} \mathbf{Q} \odot \tilde{\nabla} \mathbf{Q} + \dots \right],$$

Non-dimensional equations – dimensionless groups

Length scale L and timescale $t_0 = \zeta_1 / (8\gamma_F)$ – hence dimensionless Q-tensor equation

$$\begin{aligned} \frac{\partial \mathbf{Q}}{\partial \tilde{t}} + \tilde{\mathbf{v}} \cdot \tilde{\nabla} \mathbf{Q} - \tilde{\Omega} \mathbf{Q} - \mathbf{Q} \tilde{\Omega} + \underbrace{\mathbf{Tu}}_{=(\zeta_2/\zeta_1)} \tilde{\mathbf{D}} \\ = \epsilon^2 \tilde{\nabla}^2 \mathbf{Q} + g_1(1-\theta) \mathbf{Q} + 3g_2 \mathbf{Q}^2 - \frac{1}{2} \text{tr}(\mathbf{Q}^2) \mathbf{Q} + \frac{1}{3} \mathbb{I} \left[\mathbf{Tu} \text{tr}(\tilde{\mathbf{D}}) - 3g_2 \text{tr}(\mathbf{Q}^2) \right], \end{aligned}$$

where

$$\alpha_F / (8\gamma_F) = -g_1 [1 - (T/T_*)] \equiv -g_1(1-\theta), \quad \beta_F / (8\gamma_F) = g_2, \quad \epsilon = k / (L^2 \gamma_F).$$

Hence also, a dimensionless momentum equation:

$$\frac{\partial \tilde{\mathbf{v}}}{\partial \tilde{t}} + \tilde{\mathbf{v}} \cdot \tilde{\nabla} \tilde{\mathbf{v}} = -\tilde{\nabla} \tilde{p} + \frac{1}{\text{Re}} \nabla \cdot \tilde{\mathbf{D}} + \text{Br} \nabla \cdot \left[-\epsilon^2 \tilde{\nabla} \mathbf{Q} \odot \tilde{\nabla} \mathbf{Q} + \dots \right],$$

where

$$\text{Br} = \frac{\zeta_1}{\rho_0 L(L/t_0)}, \quad \text{Re} = \frac{\rho_0 L(L/t_0)}{\zeta_3}.$$

Limiting case

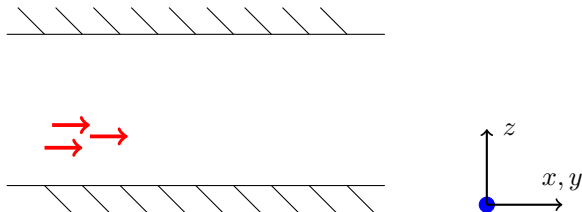
I work on the limit where $Br = 0$ – no feedback of Q-tensor gradients into the flow – flow is independent of Q-tensor. I can therefore apply **standard chaotic flows** to the Q-tensor dynamics

$$\begin{aligned} \frac{\partial \mathbf{Q}}{\partial \tilde{t}} + \tilde{\mathbf{v}} \cdot \tilde{\nabla} \mathbf{Q} - \tilde{\boldsymbol{\Omega}} \mathbf{Q} - \mathbf{Q} \tilde{\boldsymbol{\Omega}} + \underbrace{\text{Tu}}_{=(\zeta_2/\zeta_1)} \tilde{\mathbf{D}} \\ = \epsilon^2 \tilde{\nabla}^2 \mathbf{Q} + g_1(1 - \theta) \mathbf{Q} + 3g_2 \mathbf{Q}^2 - \frac{1}{2} \text{tr}(\mathbf{Q}^2) \mathbf{Q} + \frac{1}{3} \mathbb{I} \left[\text{Tu tr}(\tilde{\mathbf{D}}) - 3g_2 \text{tr}(\mathbf{Q}^2) \right], \end{aligned}$$

The **flow timescales** and the **tumbling parameter** Tu are the key parameters.

Two-dimensional geometry

I work with a sample confined between two narrowly separated parallel plates. **Anchoring conditions** are applied in the same fashion at the top and bottom walls such that the director is parallel to the plates.



As such, the Q-tensor simplifies:

$$\mathbf{Q} = \begin{pmatrix} q & r & 0 \\ r & s & 0 \\ 0 & 0 & -(q+s) \end{pmatrix} \quad \mathcal{S} = \sqrt{6\text{tr}(\mathbf{Q}^2)} = \sqrt{12(r^2 + q^2 + s^2 + qs)}.$$

The dynamical equations for the Q-tensor also simplify – there are only three of them.

Fixed-point analysis

I look at fixed points for $\mathbf{v} = \nabla = \partial_t = 0$. Remarkably, all fixed points can be found in closed form (not shown) and classified:

Fixed-point analysis

I look at fixed points for $\mathbf{v} = \nabla = \partial_t = 0$. Remarkably, all fixed points can be found in closed form (not shown) and classified:

- Biaxial state – two independent eigendirections in a spectral decomposition of Q
- Uniaxial state - only one independent eigendirection \hat{n} , with $Q_{ij} \propto n_i n_j - (1/3)\delta_{ij}$

Fixed-point analysis

I look at fixed points for $\mathbf{v} = \nabla = \partial_t = 0$. Remarkably, all fixed points can be found in closed form (not shown) and classified:

- Biaxial state – two independent eigendirections in a spectral decomposition of Q
- Uniaxial state – only one independent eigendirection \hat{n} , with $Q_{ij} \propto n_i n_j - (1/3)\delta_{ij}$

Hence,

- Case 1a ($r = 0, s = q$) gives a stable most-dangerous mode (MDM) – **biaxial**
- Case 1b,c ($r = 0, s \neq q$) give neutral and unstable MDMs – **uniaxial**
- Case 2 gives neutral and unstable MDMs – **uniaxial**

Fixed-point analysis – one last subtlety

Another possibility – Case 3, with $s(t) = \lambda q(t)$, where $\lambda = \text{Const}$. Dynamics collapse into a single equation

$$\frac{dq}{dt} = \Phi(q), \quad r^2 = (2\lambda^2 + 5\lambda + 2)q^2$$

This gives more stable uniaxial fixed points which are all stable. These fixed points agree with Case 1b,c and Case 2 fixed points yet Case 3 is stable while the others are not – Case 3 is a restriction of other cases along **stable eigendirections**.

Numerics without flow

To understand evolution, I study Q-tensor dynamics (three-equation model) in the absence of flow using a pseudospectral numerical method on a doubly-periodic spatial domain. Two sets of initial conditions considered:

- Uni-axial initial conditions $\hat{n} = (\cos \varphi, \sin \varphi)$, with a different random number φ and a different random value of the scalar order parameter \mathcal{S} at each point in space:

$$\mathbf{Q}(t=0) = \mathbf{Q} = \frac{1}{2}\mathcal{S} \begin{pmatrix} \cos^2 \varphi - 1/3 & \cos \varphi \sin \varphi & 0 \\ \cos \varphi \sin \varphi & \sin^2 \varphi - 1/3 & 0 \\ 0 & 0 & -1/3 \end{pmatrix}$$

- Bi-axial initial conditions, with

$$\mathbf{Q}(t=0) = \begin{pmatrix} \lambda_1 n_x^2 + \lambda_2 n_y^2 & (\lambda_1 - \lambda_2)n_x n_y & 0 \\ (\lambda_1 - \lambda_2)n_x n_y & \lambda_1 n_y^2 + \lambda_2 n_x^2 & 0 \\ 0 & 0 & -(\lambda_1 + \lambda_2) \end{pmatrix}$$

with λ_1 and λ_2 drawn from uniform distributions such that $\text{tr}[\mathbf{Q}(t=0)] = 0$.

Results – Uniaxial initial conditions

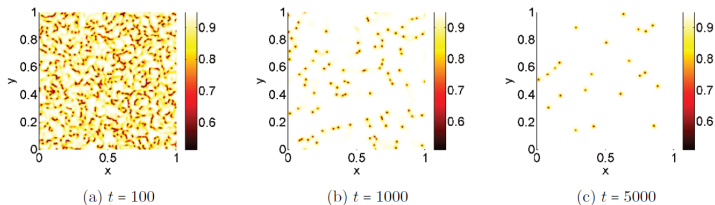


FIG. 1. Snapshots of scalar order parameter at various times.

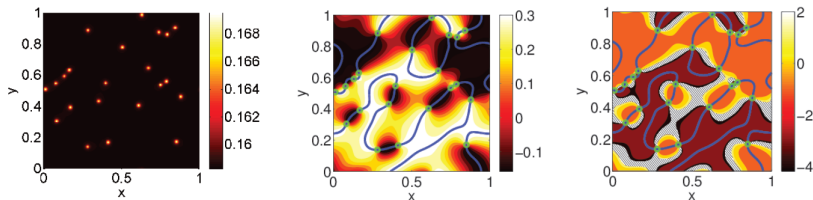
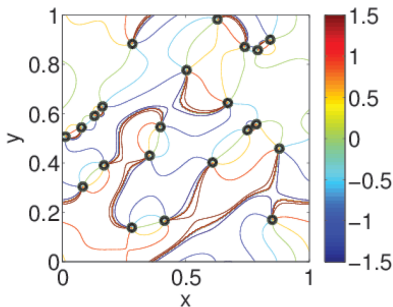


FIG. 2. Fuller characterization of the system at $t = 5,000$. (a) Plot of $s + q$ at $t = 5000$ revealing a bimodal distribution. The value $s + q \approx A_+$ corresponds to a type-3 stable fixed point while the $s + q \approx 2(A_+ - g_2)$ corresponds to a type-1(a) unstable bi-axial fixed point; (b) Plot of s at the same time. The small circular contours correspond $s + q \approx 2(A_+ - g_2)$ (i.e. bi-axial regions) and the larger contours correspond to $r = 0$; (c) Plot of $\lambda = s/q$ for $|q| > 0.05$ (the hatched regions correspond to $|q| < 0.05$).

Defects

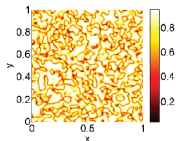
Why do unstable biaxial fixed points persist at late times?

- Answer is due to defects – director $\hat{n} = (\cos \varphi, \sin \varphi)$ experiences jumps in φ (line defects).
- Line defects end at defect **cores**, which coincide with biaxial islands.
- Each defect core has a topological charge (winding number) $\pm 1/2$.
- Total topological charge is conserved, meaning biaxial islands can't spontaneously disappear – they have to **merge**, thereby gradually reducing system energy.

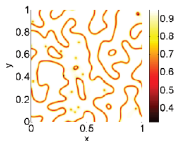


Results – Biaxial initial conditions

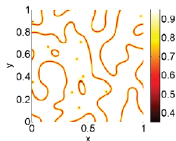
The system forms domains – pure stable biaxial fixed points or mixed domains containing uniaxial fixed points and unstable biaxial islands:



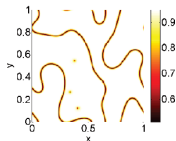
(a) $t = 100$



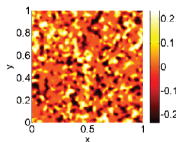
(b) $t = 1000$



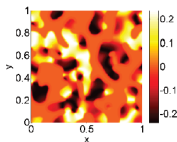
(c) $t = 2000$



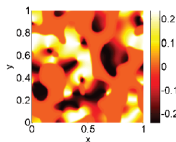
(d) $t = 5000$



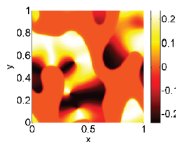
(e) $t = 100$



(f) $t = 1000$



(g) $t = 2000$



(h) $t = 5000$

Top: snapshots of scalar order parameter at various times for the bi-axial initial data.
Bottom: corresponding snapshots for r . The domains with $r = 0$ correspond to the bi-axial state.

Coarsening

Simulations show that system self-orders over time – random initial conditions coalesce into domains.

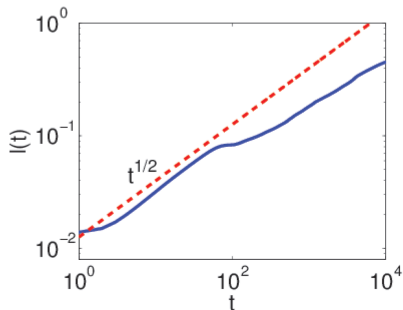
Quantified by measuring

$$L(t) = 2\pi/k_1, \quad k_1 = \frac{\int |\widehat{C}_{\mathbf{k}}|^2 d^2k}{\int |\mathbf{k}|^{-1} |\widehat{C}_{\mathbf{k}}|^2 d^2k},$$

where

$$\langle \mathcal{S} \rangle = \frac{1}{|\Omega|} \int_{\Omega} \mathcal{S}(\mathbf{x}) d^2x,$$

$$\widehat{C}_{\mathbf{k}} = \int_{\Omega} e^{-i\mathbf{x}\cdot\mathbf{k}} (\mathcal{S} - \langle \mathcal{S} \rangle) d^2x.$$



Calculation shows $L(t) \sim t^{1/2}$
– **diffusive scaling**

Not the same L as before – sorry!

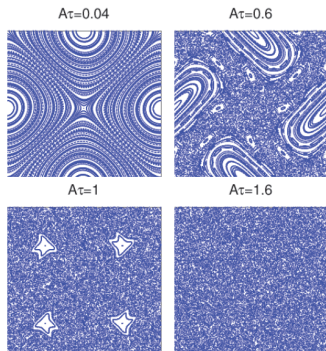
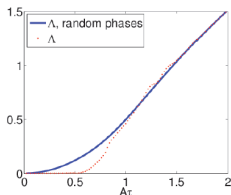
Model sine flow

I first of all looked at a model (quasi-) periodic velocity field,

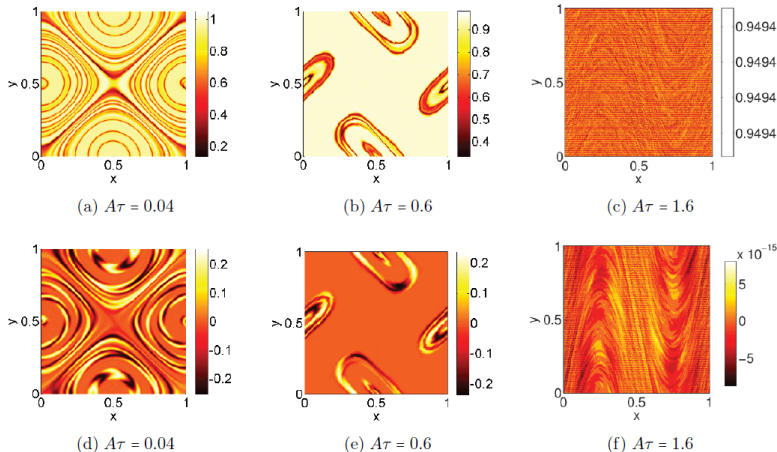
$$\begin{aligned}u &= A \sin(k_0 y + \varphi_n), & 0 \leq \text{mod}(t, \tau) < \frac{1}{2}\tau, \\v &= A \sin(k_0 x + \psi_n), & \frac{1}{2}\tau \leq \text{mod}(t, \tau) < \tau,\end{aligned}$$

which mimics the effect of turbulence at high Prandtl number.

- The phases φ_n and ψ_n are held constant or are randomized periodically.
- The velocity field has a Lagrangian timescale given by the Lyapunov exponent Λ , which can be computed for the constant-phase and random-phase cases.

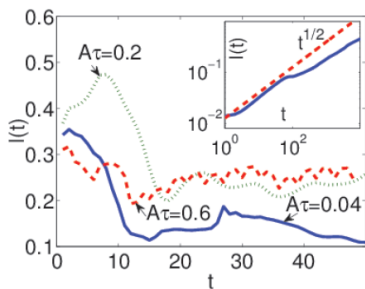


Results – no tumbling, constant-phase sine flow

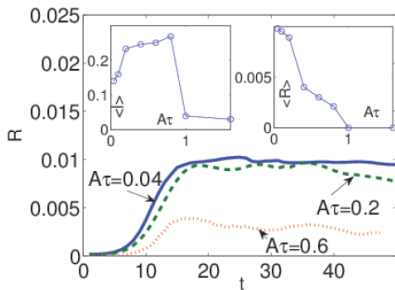


Across the top: snapshots of scalar order parameter at various times for various values of $A\tau$, with $Tu = 0$. Across the bottom: corresponding snapshots of r . Snapshots in the first two columns are taken at $t = 320$. The third column (figures (c) and (f)) concerns $A\tau = 1.6$, for which the snapshots are taken at $t = 320$; these are included here to demonstrate the relaxation to a uniform state for the large values of $A\tau$. The compressed colour bars in these figures is a consequence of the rapid relaxation to the uniform steady state.

Coarsening is arrested / overwhelmed



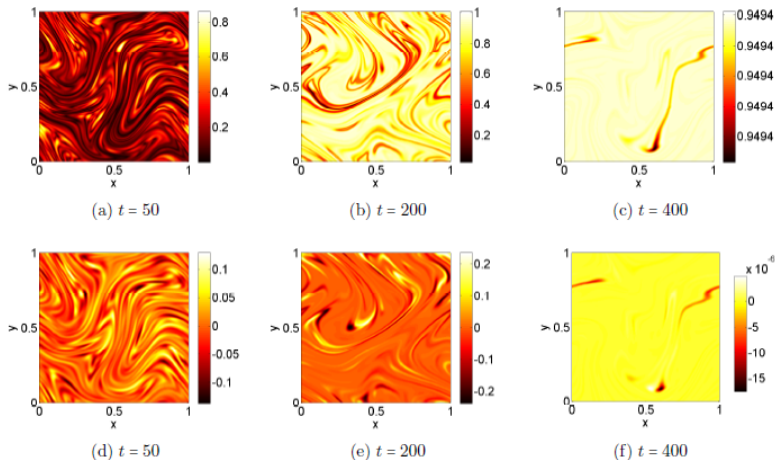
(a)



(b)

(a) Time evolution of the domain scale $L(t)$ for various values of $A\tau$. The inset shows the time-averaged values of $L(t)$ for a much larger range of $A\tau$ -values, with angle brackets denoting a time average. The time-averages are taken over intervals where the Q -tensor dynamics are in a statistically steady state. (b) The same, for $R := L_x^{-1} L_y^{-1} \iint r^2 dx dy$

Results – Only the biaxial fixed point remains when the phases are randomized



Across the top: snapshots of scalar order parameter at various times for $A\tau = 0.04$ and $Tu = 0$, for the random-phase sine flow. Across the bottom: corresponding snapshots of r . The compressed colour bars in panel (c) is a consequence of the rapid relaxation to the uniform steady state.

The oscillating cell flow

I also consider an oscillating cell flow with $u = \partial\psi/\partial y$ and $v = -\partial\psi/\partial x$, where $\psi(x, y, z)$ is the time-dependent streamfunction

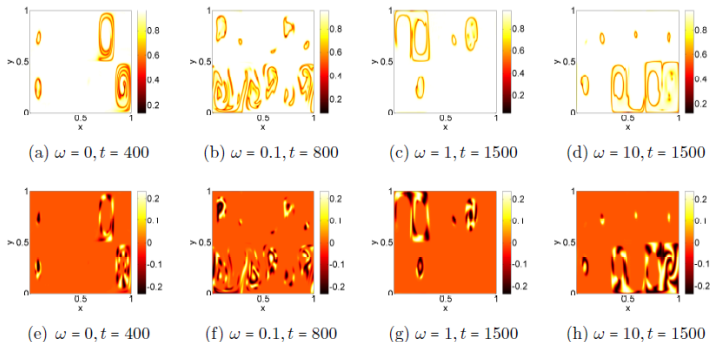
$$\psi(x, y, z, t) = A_0 \sin(k_x x + A_1 \cos(\omega t)) \sin(k_y y).$$

The oscillating cell flow

I also consider an oscillating cell flow with $u = \partial\psi/\partial y$ and $v = -\partial\psi/\partial x$, where $\psi(x, y, z)$ is the time-dependent streamfunction

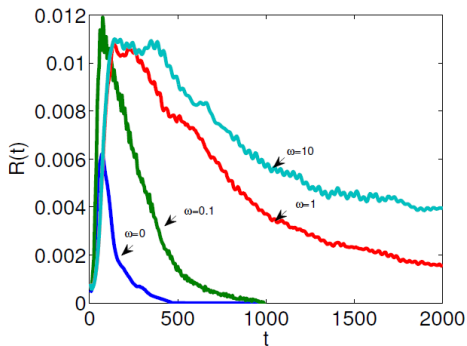
$$\psi(x, y, z, t) = A_0 \sin(k_x x + A_1 \cos(\omega t)) \sin(k_y y).$$

Again, only biaxial fixed point survives:



Across the top: snapshots of scalar order parameter for various values of ω and for $Tu = 0$, for the oscillating cell flow. Across the bottom: corresponding snapshots of r .

Relaxation to the biaxial state depends on the frequency of the oscillating cell flow.



Time evolution of $R(t)$ for various values of ω , for the oscillating cell flow whose stream-function is given by Equation (24). Flow parameters: $A_0 = 0.05/(2\pi)$, $A_1 = \pi$, $k_x = 6\pi/L_x$, $k_y = 2\pi/L_y$, with $L_x = L_y = 1$. The simulations again use periodic boundary conditions in both spatial directions.

Discussion

Key to understanding depends on studying dynamics along Lagrangian trajectories:

$$\frac{d}{dt} \begin{pmatrix} q \\ r \\ s \end{pmatrix} = \begin{pmatrix} F_1(q, r, s) \\ F_2(q, r, s) \\ F_3(q, r, s) \end{pmatrix} + \begin{pmatrix} 2r\Omega_{12} \\ \Omega_{12}(s - q) \\ -2r\Omega_{12} \end{pmatrix}, \quad \text{Tu} = 0, \\ \text{(Diffusion negligible)}$$

Discussion

Key to understanding depends on studying dynamics along Lagrangian trajectories:

$$\frac{d}{dt} \begin{pmatrix} q \\ r \\ s \end{pmatrix} = \begin{pmatrix} F_1(q, r, s) \\ F_2(q, r, s) \\ F_3(q, r, s) \end{pmatrix} + \begin{pmatrix} 2r\Omega_{12} \\ \Omega_{12}(s - q) \\ -2r\Omega_{12} \end{pmatrix}, \quad \text{Tu} = 0, \quad (\text{Diffusion negligible})$$

- Constant-phase sine flow:

- ▶ For $A\tau \ll 1$ replace Ω_{12} with averaged value along trajectories. Average value $\langle \Omega_{12} \rangle$ is zero in **extended regions**, for $A\tau \ll 1$ - domain structures 'frozen in' to flow and biaxial AND mixed bi/uniaxial regions observed.
- ▶ For $A\tau \gg 1$ fluid parcels experience instantaneous value of Ω_{12} - only biaxial fixed point survives.

Discussion

Key to understanding depends on studying dynamics along Lagrangian trajectories:

$$\frac{d}{dt} \begin{pmatrix} q \\ r \\ s \end{pmatrix} = \begin{pmatrix} F_1(q, r, s) \\ F_2(q, r, s) \\ F_3(q, r, s) \end{pmatrix} + \begin{pmatrix} 2r\Omega_{12} \\ \Omega_{12}(s - q) \\ -2r\Omega_{12} \end{pmatrix}, \quad \text{Tu} = 0, \quad (\text{Diffusion negligible})$$

- Constant-phase sine flow:

- ▶ For $A\tau \ll 1$ replace Ω_{12} with averaged value along trajectories. Average value $\langle \Omega_{12} \rangle$ is zero in **extended regions**, for $A\tau \ll 1$ - domain structures 'frozen in' to flow and biaxial AND mixed bi/uniaxial regions observed.
- ▶ For $A\tau \gg 1$ fluid parcels experience instantaneous value of Ω_{12} - only biaxial fixed point survives.

- For random-phase sine flow, Lagrangian average $\langle \Omega_{12} \rangle$ is zero but not in extended regions (fully chaotic flow) - diffusion destroys any mixed regions - only biaxial fixed point remains.

Discussion

Key to understanding depends on studying dynamics along Lagrangian trajectories:

$$\frac{d}{dt} \begin{pmatrix} q \\ r \\ s \end{pmatrix} = \begin{pmatrix} F_1(q, r, s) \\ F_2(q, r, s) \\ F_3(q, r, s) \end{pmatrix} + \begin{pmatrix} 2r\Omega_{12} \\ \Omega_{12}(s - q) \\ -2r\Omega_{12} \end{pmatrix}, \quad \text{Tu} = 0, \quad (\text{Diffusion negligible})$$

- Constant-phase sine flow:

- ▶ For $A\tau \ll 1$ replace Ω_{12} with averaged value along trajectories. Average value $\langle \Omega_{12} \rangle$ is zero in **extended regions**, for $A\tau \ll 1$ - domain structures 'frozen in' to flow and biaxial AND mixed bi/uniaxial regions observed.
- ▶ For $A\tau \gg 1$ fluid parcels experience instantaneous value of Ω_{12} - only biaxial fixed point survives.

- For random-phase sine flow, Lagrangian average $\langle \Omega_{12} \rangle$ is zero but not in extended regions (fully chaotic flow) - diffusion destroys any mixed regions - only biaxial fixed point remains.
- Oscillating cell flow - very different from random-phase sine flow but explanation is the same.

Discussion and Conclusions

- We have formulated a theory for flow and liquid-crystal dynamics in a planar system.

Discussion and Conclusions

- We have formulated a theory for flow and liquid-crystal dynamics in a planar system.
- No backreaction – **passive advection**

Discussion and Conclusions

- We have formulated a theory for flow and liquid-crystal dynamics in a planar system.
- No backreaction – **passive advection**
- Identified fixed points and their stability analytically

Discussion and Conclusions

- We have formulated a theory for flow and liquid-crystal dynamics in a planar system.
- No backreaction – **passive advection**
- Identified fixed points and their stability analytically
- For a chaotic flow without tumbling, the fixed points determine the result, with rapidly-varying flows admitting a variety of fixed points (slowly-varying flows only admit the biaxial one)

Discussion and Conclusions

- We have formulated a theory for flow and liquid-crystal dynamics in a planar system.
- No backreaction – **passive advection**
- Identified fixed points and their stability analytically
- For a chaotic flow without tumbling, the fixed points determine the result, with rapidly-varying flows admitting a variety of fixed points (slowly-varying flows only admit the biaxial one)
- With tumbling, Q -tensor morphology follows the flow (source term)

Discussion and Conclusions

- We have formulated a theory for flow and liquid-crystal dynamics in a planar system.
- No backreaction – **passive advection**
- Identified fixed points and their stability analytically
- For a chaotic flow without tumbling, the fixed points determine the result, with rapidly-varying flows admitting a variety of fixed points (slowly-varying flows only admit the biaxial one)
- With tumbling, Q -tensor morphology follows the flow (source term)
- These insights provide ways of controlling the morphology with stirring

Discussion and Conclusions

- We have formulated a theory for flow and liquid-crystal dynamics in a planar system.
- No backreaction – **passive advection**
- Identified fixed points and their stability analytically
- For a chaotic flow without tumbling, the fixed points determine the result, with rapidly-varying flows admitting a variety of fixed points (slowly-varying flows only admit the biaxial one)
- With tumbling, Q -tensor morphology follows the flow (source term)
- These insights provide ways of controlling the morphology with stirring
- Apply known techniques to the reduced planar model:
 - ▶ Bounds and *a priori* estimates
 - ▶ Lubrication theory
 - ▶ DNS of the fully coupled system – **the backreaction will be back!**